Thermochimica Acta, 136 (1988) 247–261
Elsevier Science Publishers B.V., Amsterdam – Printed in The Netherlands

THERMAL AND MÖSSBAUER STUDIES OF IRON-CONTAINING HYDROUS SILICATES. VII. GLAUCONITE

K.J.D. MACKENZIE, C.M. CARDILE and I.W.M. BROWN
Chemistry Division, DSIR, Private Bag, Petone (New Zealand)

(Received 4 February 1988)

ABSTRACT

Thermal analysis, X-ray diffraction and Mössbauer spectroscopic studies of four purified glauconites suggest that the unheated minerals have monoclinic layer-lattice structures in which both the *cis*- and *trans*-octahedral sites can be occupied. On heating below 300 °C, mechanically-held water is lost and fully oxidised ferric glauconite is formed. Dehydroxylation at ~ 300–600 °C is accompanied by changes in the Mössbauer spectra which suggest that the octahedral cations assume a mixture of four- five- and distorted six-fold coordination. The structure of glauconite dehydroxylate and its formation mechanism are discussed. Heating to higher temperatures induces increased lattice disorder, until the appearance at ~ 1000 °C of a cubic phase with X-ray and Mössbauer characteristics typical of $MgFe_2O_4$. Haematite and a glassy phase appear additionally at ~ 1200 °C.

INTRODUCTION

Glauconite is generally described as a member of the dioctahedral mica group, which differs from muscovite by having a significant proportion of the octahedral sites occupied by divalent ions (Mg^{2+} and Fe^{2+}), resulting in a generalised structural formula of

$$(K,Na,Ca)_{1.2-2.0}(Fe^{3+},Al,Fe^{2+},Mg)_{4.0}[Si,Al]_{8.0}O_{20}(OH)_4 \cdot nH_2O$$

Glauconites are formed almost exclusively in marine environments, their iron contents (typically 15–20%) giving the bluish-green colour from which they derive their name (Greek *glaucos*, bluish-green). Although glauconites are dioctahedral minerals, their X-ray powder patterns are more like those of trioctahedral biotites. Furthermore, since glauconites tend to be fine-grained, they are sometimes classified as clay minerals and grouped with the illites; a recent Mössbauer study [1] confirms that in terms of their cation environments, glauconites resemble illites, and may be considered as intermediate between montmorillonites and the iron-rich nontronites.

Thermal analyses reported for a number of glauconites indicate that the hydration water is endothermically lost on heating at 120–140 °C [2–6], with endothermic dehydroxylation occuring at 480–750 °C [2–6]. A third endothermic event at 880–995 °C [3,5], reported to occur only in mixed

0040-6031/88/$03.50

montmorillonite–glauconite minerals, but not in minerals with the perfect 1M-type structure [3], has been attributed to the formation of a new phase, identified by X-ray diffraction as magnesioferrite [5]. A combination of thermal analysis and simultaneous magnetic measurements suggests that when formed in vacuo, the dehydroxylated phase is Fe_3O_4 rather than Fe_2O_3, since its Curie point is 560 °C [7]. The mechanism of magnetite formation in vacuo in dioctahedral Fe^{2+}-containing minerals such as glauconite is envisaged [8] as

$$3Fe^{2+} + 6OH^- \rightarrow Fe_3O_4 + 2H_2O + H_2 \quad (1)$$

Although a number of Mössbauer studies of glauconite have been reported for samples from many locations [9–23], only one investigation has been reported of the phases formed in heated glauconite [24]; in samples heated at > 800 °C, a double-sextet and two central doublets were found, respectively identified as magnetite with a superparamagnetic component [24].

A major problem in many of the previous glauconite studies has been the difficulty of separating the pure mineral from numerous coexisting phases. The present work was made possible by the availability of four different samples which had been purified particularly carefully. The aim was to study aspects of the thermal decomposition sequence in air, paying special attention to the changes accompanying the oxidation of Fe^{2+}, and to the nature of the dehydroxylated phase.

EXPERIMENTAL

One of the four glauconites studied, labelled CHA, was separated from submarine phosphorite granules collected from the Chatham Rise, off the east coast of the South Island of New Zealand; the others (labelled OAM2, OAM7 and OAM8) were from sedimentary deposits from Oamaru, New Zealand. The glauconite component was isolated and separated from contaminants of aragonite, calcite, siderite, plagioclase, quartz and finely-divided goethite by a series of physical and chemical treatments described elsewhere [25]. The chemical analyses and structural formulae of the purified materials are given in Table 1.

X-ray powder diffraction was unable to detect any remaining crystalline contaminants, and indicates that the samples are all well-ordered monoclinic glauconites.

Thermal analyses (DTA, TG and EGA) were carried out in air at a heating rate of 10 °C min^{-1}, as described elsewhere [26]. X-ray diffraction and Mössbauer spectroscopy were then used to study samples heated to progressively higher temperatures in platinum-lined ceramic boats for 15 min in air. The X-ray diffractometer was a computer-controlled Philips PW1700 using Co $K\alpha$ radiation and a graphite monochromator. For accurate measurements of the 060 reflection, elemental Si was used as the

TABLE 1

Chemical analyses and unit cell contents of the glauconites calculated on the basis of 24 (O, OH). (Fe^{2+}/Fe^{3+} ratios estimated by Mössbauer spectroscopy.)

Element		CHA (%)		OAM2 (%)		OAM7 (%)		OAM8 (%)	
SiO_2		47.21		49.84		47.78		46.60	
Al_2O_3		7.06		6.34		6.86		7.64	
Fe_2O_3		20.11		26.19		25.43		26.30	
MgO		4.81		2.56		2.67		2.49	
CaO		1.44		0.07		0.04		0.04	
Na_2O		0.10		0.05		1.35		1.08	
K_2O		6.98		7.28		6.39		6.36	
TiO_2		0.06		0.07		0.27		0.26	
$H_2O(-)$		7.8		3.6		5.1		4.9	
$H_2O(+)$		4.4		4.0		4.1		4.3	
Total		99.97		100.00		99.99		99.97	
Unit cell contents									
Si	Tet.	7.32	8.0	7.42	8.0	7.26	8.0	7.08	8.0
Al		0.60		0.32		0.56		0.82	
Fe^{3+}		0.08		0.26		0.18		0.10	
Al	Oct.	0.68	4.06	0.80	4.04	0.66	4.02	0.56	4.08
Mg		1.12		0.56		0.60		0.56	
Fe^{3+}		1.98		2.30		2.34		2.62	
Fe^{2+}		0.28		0.38		0.38		0.30	
Ti		–		–		0.04		0.04	
K	Exch.	1.38	1.64	1.38	1.42	1.24	1.64	1.24	1.56
Na		0.02		0.02		0.40		0.32	
Ca		0.24		0.02		–		–	
O		20		20		20		20	
(OH)		4		4		4		4	

Analyst, R.L. Goguel.

Tetrahedral Fe^{3+} contents estimated by Mössbauer spectroscopy taken from ref. 25.

angular calibrant. The Mössbauer spectra were obtained at room temperature using an Elscint AME-50 spectrometer with a Co–Rh source, the velocity scale being referenced to soft iron. The spectra were computer-fitted with a number of overlapping Lorentzian peak lineshapes using a non-linear regression χ^2 minimisation procedure.

RESULTS AND DISCUSSION

Thermal analysis and X-ray diffraction

The thermal analysis curves for the four glauconites are shown in Fig. 1. All samples underwent endothermic water loss below 120 °C, followed by

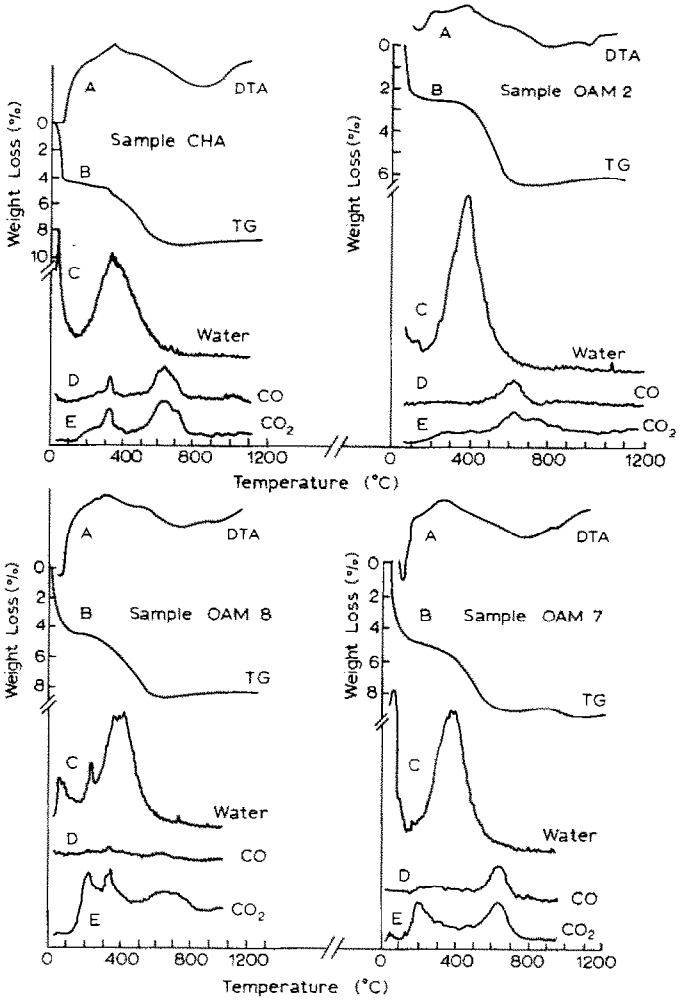

Fig. 1. Thermal analysis curves for four glauconites. Heating rates, 10 °C min^{-1} in air (DTA and TG) and 10 °C min^{-1} in He (EGA).

dehydroxylation at about 300–700 °C. The TG and mass 17 (water) EGA curves of samples CHA, OAM2 and OAM7 show no evidence of multi-stage dehydroxylation as reported by Logvinenko et al. [4] under quasi-equilibrium conditions. By contrast, the mass 17 EGA curve for sample OAM8 suggests that water loss in the dehydroxylation temperature range may occur in up to three stages (Fig. 1). The DTA curves of all samples lack the conspicuous dehydroxylation endotherm, probably because of the counteracting effect of exothermic Fe^{2+} oxidation, which commences just prior to dehydroxylation (see next section). One or more broad weak endotherms which occur at higher temperatures as previously reported [3,5] appear to be related to the formation of the high-temperture phases, but only in OAM7

are these associated with a small weight change, which may reflect some oxidation to haematite (Fe_2O_3).

The only other evolved gas species detected by mass spectrometry are small quantities of CO and CO_2 (Fig. 1). These could originate either from small amounts of residual carbonate contaminants, or from residual organic acid which may remain from the purification procedures despite repeated washing. The thermal decomposition product of carbonate contaminants is principally CO_2, with only small amounts of CO resulting from cracking in the mass spectrometer; decomposition of carboxylic acids produces both CO and CO_2 as primary products. On this basis, the CO/CO_2 ratios in samples CHA and OAM2 appear to be more consistent with organic acid contaminants, whereas OAM8 probably contains trace carbonate contaminants only. In OAM7, a low-temperature CO_2 evolution is not accompanied by significant CO and probably arises from carbonate, whereas the evolution of both CO and CO_2 at about 650 °C suggests the additional presence of residual organic acid. However, the amounts of contaminants in all samples

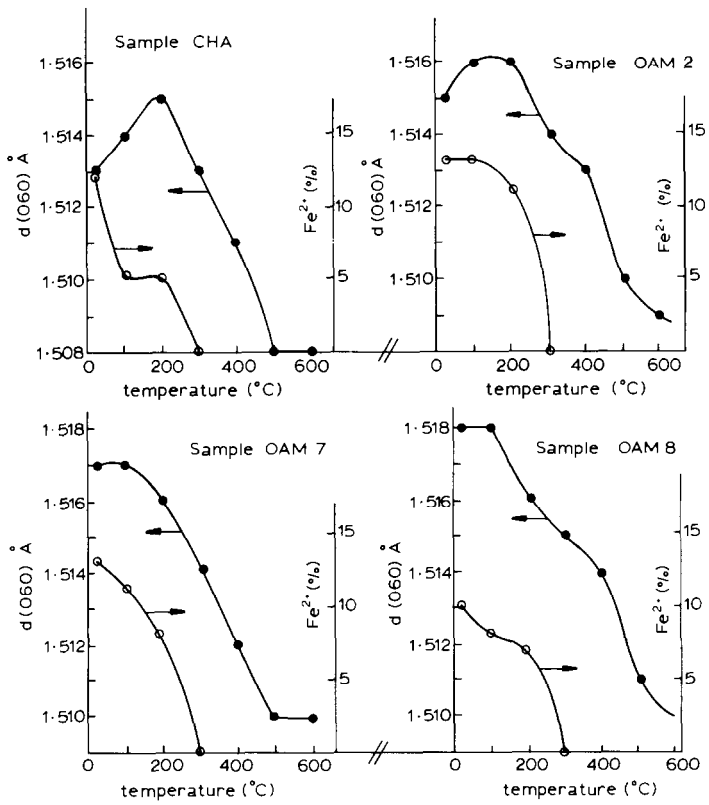

Fig. 2. Change in the 060 spacing and total Fe^{2+} content (estimated by Mössbauer spectroscopy) as a function of heating temperature for four glauconites.

are very small, and are unlikely to influence the thermal decomposition of the bulk clay mineral.

The thermal elimination of hydroxyl water and the concomitant oxidation of Fe^{2+} (see next section) are accompanied by only small changes in the X-ray pattern of the glauconite, principally in the 060 reflection, which is sensitive to changes in the *b* axis of the unit cell. The measured 060 spacings are shown as a function of heating temperature in Fig. 2. All samples show a progressive decrease in the 060 spacing during dehydroxylation, preceded in samples CHA and OAM2 by a small increase in the spacing below 200 °C. The Fe^{2+} content at each temperature, estimated from Mössbauer measurements (see next section), is also indicated in Fig. 2, and suggests that the major changes in the 060 spacing (above 200 °C) are more a consequence of dehydroxylation than of iron oxidation, which is complete between 200 and 300 °C.

The X-ray pattern of glauconite dehydroxylate persists in all samples up to 800 °C but, by 900 °C, the dehydroxylate peaks have begun to be replaced by those of a poorly-ordered spinel resembling magnetite, Fe_3O_4, without the intervention of a truly X-ray amorphous state. The crystallinity of the new phase improves sufficiently on heating above 1000 °C for a precise determination to be made of its *a* parameter, which ranges between 8.373 and 8.375 Å in the various samples. These measurements indicate that the high-temperature product is not magnetite as suggested by Escoubes et al. [7], for which $a = 8.396$ Å (JCPDS card no 19-629), but more nearly approaches low magnesioferrite, $MgFe_2O_4$ ($a = 8.375$ Å, JCPDS card no. 17-464), as reported by Utsal and Utsal [5]. At 1200 °C, a small amount of haematite is the only other detectable crystalline phase, but a broad X-ray diffraction hump centred at about 4.7 Å indicates the presence of a significant amount of glass formed from the silica and alkali components of the original glauconite.

Mössbauer spectroscopy

Typical room-temperature Mössbauer spectra are shown in Fig. 3. Although the spectrum of unheated glauconite (Fig. 3A) appears fairly simple, there has been much previous debate as to the way in which it should be interpreted. The octahedral cation sites in the structure are associated with hydroxyl groups either in a *cis*-configuration (hydroxyls adjacent) or in a *trans*-configuration (hydroxyls opposite). The structure contains one *trans*-site and two *cis*-sites, any of which may be occupied by either Fe^{2+} or Fe^{3+} ions; in addition, the possibility of Fe^{3+} occupying tetrahedral sites [1,25] or interlayer positions [17,21] has been recognised. Thus, spectra have been fitted with one Fe^{3+} and one Fe^{2+} doublet [20,22], two Fe^{3+} and one Fe^{2+} [9,10,20], one Fe^{3+} and two Fe^{2+} [11,20], two Fe^{3+} and two Fe^{2+} [13,16,18–20], two Fe^{3+} (including one tetrahedral site) [14], three Fe^{3+} and

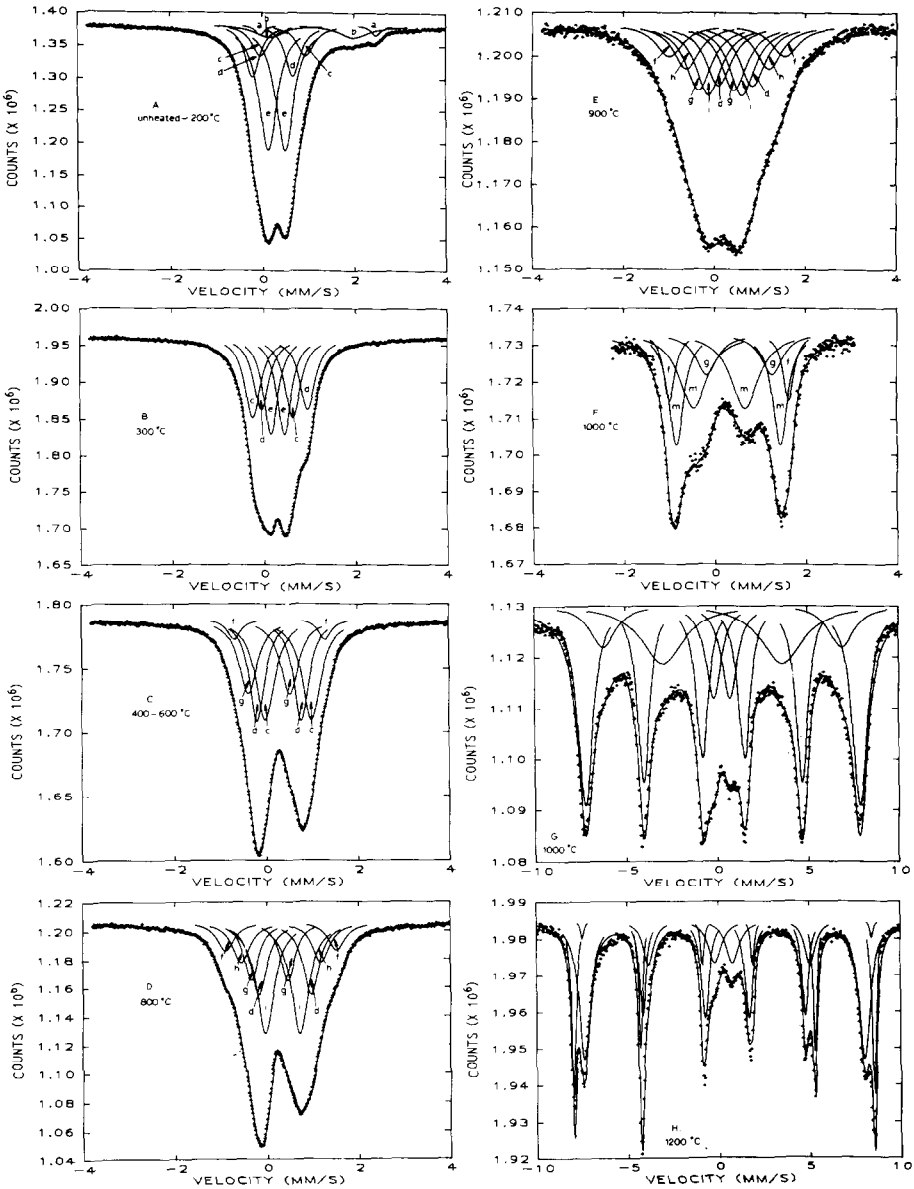

Fig. 3. Typical room-temperature Mössbauer spectra of unheated and heated glauconite (sample OAM2). Letters a–i identify resonances referred to in Fig. 4 and in the text; m = $MgFe_2O_4$.

one Fe^{2+} [23], three Fe^{3+} (including one interlayer site) plus two Fe^{2+} [17,21], five Fe^{3+} (including one tetrahedral site) [12] and four Fe^{3+} plus three Fe^{2+} [22]. It is generally agreed in the literature that the *cis*-sites and *trans*-sites can be distinguished, with the *cis*-Fe^{3+} quadrupole splitting (QS) values smaller than the *trans*-Fe^{3+} QS, by contrast with the *cis*-Fe^{2+} QS

values which are larger than those of the *trans*-Fe^{2+} sites [11,15–19,21,25]. However, there is little agreement about the assignment of the additional sites which have to be included to give a satisfactory fit to better quality spectra; in some cases an Fe^{3+} site has been fitted which has clearly tetrahedral parameters [1,25], but other additional Fe^{3+} doublets have been assigned either to the second *cis*-site [25] or to iron in interlayer sites [17,21].

For the present purpose, both the unheated and heated spectra were fitted to no more than three Fe^{3+} and two Fe^{2+} doublets. Fewer doublets gave a significantly poorer fit, judged both by the χ^2 test and visually, whereas the fitting of more than five doublets, while giving a small improvement in χ^2, unnecessarily obscures the behaviour of the iron during heating. By analogy with previous assignments, the Fe^{2+} doublets a and b of the present spectra were taken to represent atoms in the *cis*-sites and *trans*-sites, respectively, with the Fe^{3+} doublets d and e assigned to *trans*-sites and *cis*-sites, respectively. According to Cardile and Brown [25], the Fe^{3+} doublet c corresponds to the second *cis*-site, although its parameters are very similar to those of a resonance described by De Grave et al. [21] as interlayer Fe^{3+}. A doublet with tetrahedral parameters was not deliberately fitted to the present spectra of the unheated glauconites, and under the minimal constraints imposed in the fitting philosophy used here, no doublet with tetrahedral parameters appeared spontaneously in the fitted spectra. This is by contrast with previous fitting philosophy [25], in which a small tetrahedral doublet was deliberately introduced and constrained until the fit had stabilised. The appearance of doublets with tetrahedral parameters in the present samples after heating was not a result of such a procedure; these doublets were located in the fitted envelope by an unconstrained fitting procedure. Their spontaneous appearance at a later stage in the reaction may simply reflect a significant increase in the spectral intensity of resonances which were present only weakly in the unheated samples.

After heating the samples to progressively higher temperatures, a number of somewhat complex changes are observed in the room-temperature Mössbauer spectra, in which the original resonances are progressively replaced by others, which in turn are replaced by spectra characteristic of the final products. The behaviour of all four glauconites is remarkably similar, engendering confidence that the results are typical of these minerals. The changes in the spectra of sample OAM7, which can be taken as representative, are plotted in Fig. 4. Of the iron species originally present, both the Fe^{2+} species represented by resonances a and b are equally readily oxidised, having disappeared by 300 °C. The Fe^{3+} resonance e, normally identified with ions in *cis*-sites, is also thermally unstable, disappearing at 300–400 °C. The other two Fe^{3+} resonances originally present (c and d) grow at the expense of a, b and e (Fig. 4A). All these reactions occur in the temperature range in which hydration water is removed but structural (hydroxyl) water remains intact; the product is thus a fully oxidised (ferric) glauconite.

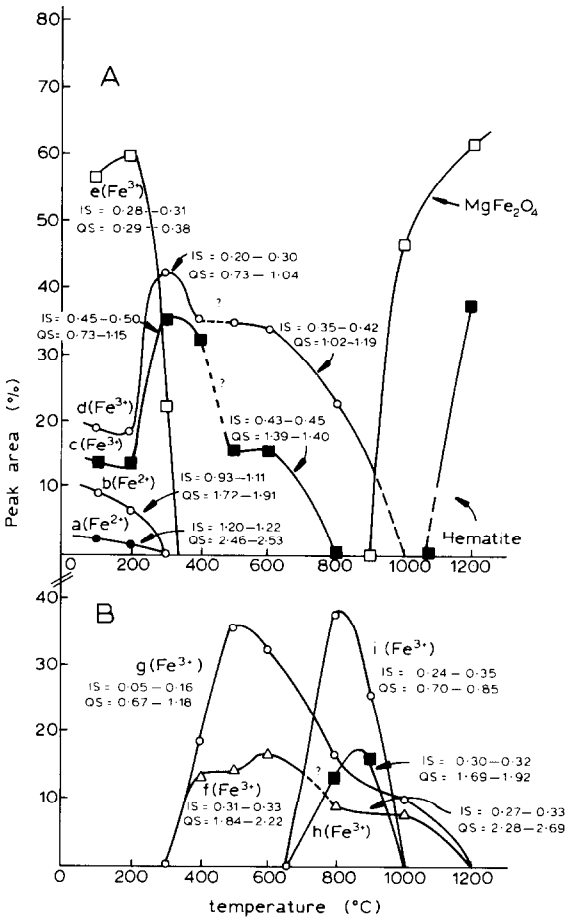

Fig. 4. Typical changes in the relative peak areas of the room-temperature Mössbauer resonances of glauconite (sample OAM7) as a function of heating temperature, assuming recoil-free fractions of Fe^{2+} and Fe^{3+} to be approximately equal. Isomer shifts quoted with respect to soft iron metal. A. Original and final resonances. B. Intermediate (transitory) resonances.

Dehydroxylation is accompanied by a marked increase in the *QS* values of resonances c and d, consistent with an increase in the distortion of these octahedral sites. The parameters of resonance d are very similar to those of an Fe^{3+} doublet found in dehydroxylated montmorillonites ($IS = 0.34–0.36$, $QS = 1.21–1.28$ mm s^{-1}) [27] and dehydroxylated muscovites ($IS = 0.36–0.46$, $QS = 1.24–1.44$ mm s^{-1}) [28], and identified by Heller-Kallai and Rozenson [29] as a five-coordinate (originally *cis*) site. Concomitantly, two new resonances, f and g, can be resolved, resonance f having parameters similar to those of Fe^{3+} in the very distorted octahedral sites of dehydroxylated montmorillonites and muscovites ($IS = 0.20–0.46$, $QS = 1.68–1.86$ mm s^{-1}) [27–29]. Thus, doublets d and f are typical of those found in the

dehydroxylates of structurally-related minerals. The new Fe^{3+} resonance g has parameters which are typically four-coordinate; such a site has been observed in the solid-state 27-Al NMR spectra of dehydroxylated montmorillonite, although the occurrence of four-coordinate iron could not be demonstrated convincingly in that material by Mössbauer spectroscopy [27]. The resolution of such a site in glauconite dehydroxylate is a consequence of its much higher iron content.

On heating to above the dehydroxylation temperature, the spectra become progressively broader until at 900 °C (Fig. 3E) the envelope is best described in terms of a number of broad doublets, typical of a disordered system containing a range of site distortions. The increased distortion in the system is also reflected by the abrupt increase in the *QS* value of doublet f (Fig. 4B). Although two additional transitory sites h and i were resolved between 800 and 1000 °C (Fig. 4B), the spectra of this stage are better considered in terms of a continuum of site energies, similar to the situation in the spectrum of unheated montmorillonite [27]. At about 1000 °C, a magnetically-split spectrum appears (Fig. 4G) with residual components of doublets f and g still resolvable in the centre of the sextet (Fig. 3F). A more satisfactory fit to the magnetic spectrum is achieved by including a second sextet (Fig. 4G), as is appropriate for spinels such as Fe_3O_4 or $MgFe_2O_4$; however, the broadness of the fitted lines indicates that at this stage the material is very poorly crystalline. By 1200 °C, the double sextet spectrum is much better resolved (Fig. 3H), from which the effective magnetic hyperfine fields (B_{eff}) of Fe^{3+} in the A and B sublattices are found to be 47.2–47.5 T and 49.6–51.2 T, respectively. These fields are in slightly better agreement with the room-temperature values reported for $MgFe_2O_4$ (46.4 and 49.6 T) [30] than for magnetite (45.8 and 49.1 T) [31], confirming the X-ray evidence that Mg^{2+} occurs in the spinel phase formed from glauconite dehydroxylate. Calculations based on the analysed MgO contents of the glauconites (Table 1) suggest that if the spinel phase is composed solely of pure $MgFe_2O_4$ it should contain ~ 36% of the total iron (for the OAM series glauconites). The rather larger proportion of the Mössbauer resonance associated with this phase (Fig. 4) may suggest either that the spinel is not pure $MgFe_2O_4$, or (more likely) that it is simply a reflection of the errors involved in such an estimate. Further improvement to the fits of the 1200 °C spectra are achieved if the presence of haematite is taken into account by the inclusion of a third sextet (Fig. 3H), the effective field of which (49.4–50.3 T) falls at the lower end of the range of fields reported for haematite [31], suggesting the possible substitution of Al in this phase [31].

The crystal structures of glauconite and its dehydroxylate

Although no crystal structure has previously been reported for glauconite, a structure published for a closely-related monoclinic mineral celadonite

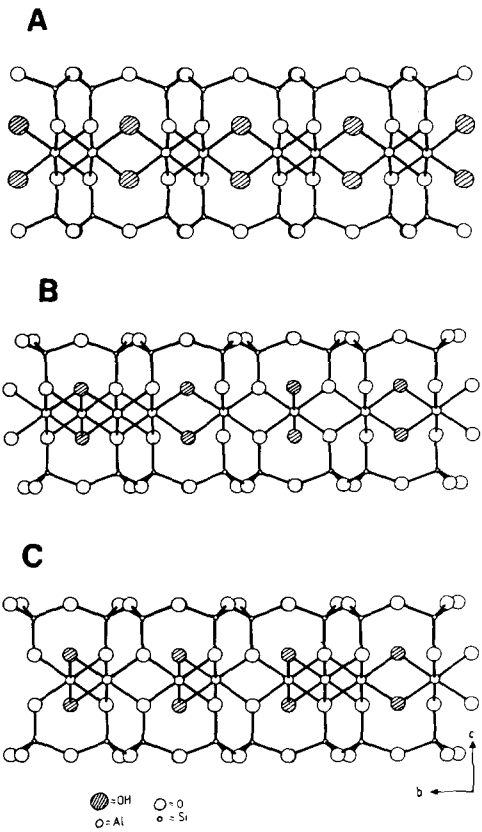

Fig. 5. Computer-generated views along the *a*-axis of various possible structural models for glauconite. A. Monoclinic celadonite structure from ref. 32 ($a = 5.23$ Å, $b = 9.05$ Å, $c = 10.15$ Å, $\beta = 100.58°$, $C2/m$). B. Based on monoclinic smectite structure from ref. 33; cation distribution from present chemical and Mössbauer analysis, assuming no tetrahedral substitution. Cell parameters as measured for sample CHA ($a = 5.259$ Å, $b = 9.078$ Å, $c = 10.191$ Å, $\beta = 100.19°$, $C2/m$). C. As for B, assuming tetrahedral substitution.

$(K,Na,Ca)_{1.76}(Fe^{3+}_{2.30}Al_{0.10}Fe^{2+}_{0.72}Mg_{0.82}Ti_{0.02})\,[Si_{7.88}Al_{0.12}]O_{20}(OH)_4$, suggests [32] that both the octahedral *cis*-sites are occupied, but not the *trans*-site (Fig. 5A). Since both *cis*-and *trans*-octahedral sites can be resolved in the Mössbauer spectra, this celadonite structure [32] does not satisfactorily describe the present glauconites. Based on electron diffraction studies of monoclinic smectites, Tsipursky and Drits [33] have identified three extremes of possible structures, differing in their occupancy of the *cis*-sites and *trans*-sites. One of these structures corresponds to the proposed celadonite structure with only *cis*-sites occupied, whereas the other two models allow varying degrees of *trans*-occupancy, and, being more appropriate to glauconite, these were examined in greater detail.

The site occupation in each glauconite was deduced from its chemical analysis, by also taking into account the Mössbauer information regarding

the partitioning of iron between the various sites. It was assumed, in the absence of evidence for cation ordering, that the octahedral Al^{3+} and Mg^{2+} partition between the sites in a similar manner to iron, and that the mineral remains dioctahedral.

A common feature of all the present glauconites is the occupation of their *trans*-sites, but the precise details of their cation configurations differ with their chemical compositions, and also depend on whether or not tetrahedral substitution is assumed. In the Mössbauer spectra of the present unheated glauconites, a previously included tetrahedral site [25] was omitted for simplicity; in a unit of 12 octahedral sites, this leads to a cation occupancy for the OAM series of glauconites of six *cis*-sites and two *trans*-sites, with four sites vacant. A computer-simulated structure satisfying these requirements is shown in Fig. 5B. On the same basis, the different chemical composition of the CHA sample predicts the occupancy of four *cis*-sites and four *trans*-sites, with four vacancies. By contrast, if account is taken of the degree of tetrahedral substitution indicated in the previously published Mössbauer study of these glauconites [25], the octahedral cation configuration of a 12-site unit approximates to the occupation of five *cis*-sites, three *trans*-sites and four vacancies. The computer-simulated structure corresponding to this situation is shown in Fig. 5C.

Structures 5B and 5C both contain *cis*-atoms in three distinguishable environments; in the two more symmetrical environments, the *cis*-atoms are adjacent to either two vacancies or two other octahedral atoms. The third, less symmetrical, situation arises where the *cis*-atom is flanked on one side by a vacancy and on the other side by another atom. According to the model of Fig. 5B, derived on the basis of the present Mössbauer data, four *cis*-atoms are located in the more symmetrical sites which should have smaller QS values, while the less symmetrical sites with larger QS values contain only two *cis*-atoms. This is in agreement with the Mössbauer results (Fig. 4) which indicate a greater occupancy of the smaller-QS *cis*-sites (resonance e) than the *cis*-sites of larger QS (resonance d).

Dehydroxylation of the glauconite structure of Fig. 5B may occur in various ways. Elimination of adjacent hydroxyl pairs a–b and c–d would result in all the octahedral cations becoming five-coordiante (Fig. 6, pathway A). In this structure, the residual oxygen atoms resulting from the elimination of H_2O from a pair of hydroxyls are retained in more or less their original positions, since shifting these atoms to median positions results in metal–oxygen bond lengths which are unrealistically small (~ 1.5 Å). Elimination of hydroxyl pairs a–d and b–c (Fig. 6, pathway B) results in the appearance of four- and six-coordinated atoms, as predicted for montmorillonite [27]. The ratio of four- to six-coordination resulting from hydroxyl elimination via pathway B is 1 : 1. The identification in the Mössbauer spectra of heated glauconites of four- five- and six-coordinate resonances (resonances g, d and f, respectively in Fig. 4) suggests that dehydroxylation

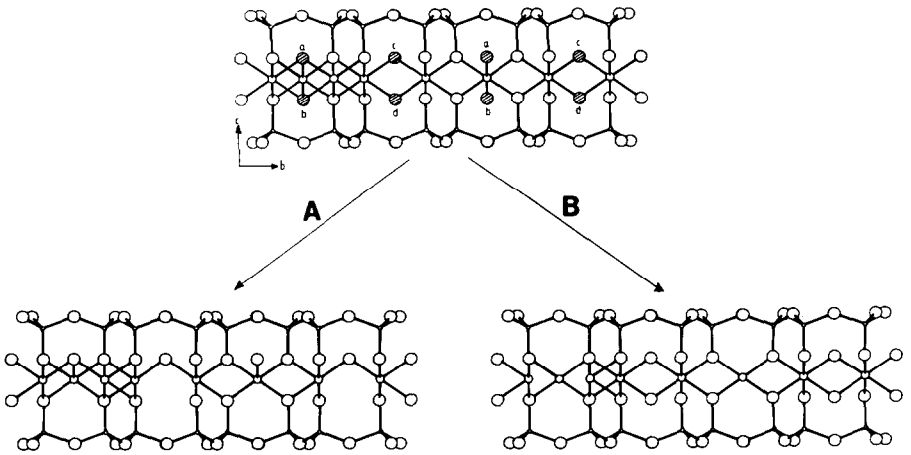

Fig. 6. Possible dehydroxylation schemes for glauconite based on computer-generated structure of Fig. 5B. Pathway A, elimination of hydroxyl pairs a–b, c–d. Pathway B, elimination of hydroxyl pairs a–d, b–c.

can occur via both pathways A and B, the structure of the dehydroxylate being a composite of both extremes. The presence of both four- and six-coordinate atoms in glauconite dehydroxylate should also facilitate the formation at higher temperatures of the spinel phase, which consists of octahedral and tetrahedral cations in a close-packed oxygen lattice.

CONCLUSIONS

1. Glauconite loses its mechanically-held water and oxidises to a fully ferric form below 300 °C. The lattice *b*-parameter, as reflected by the 060 spacing, changes slightly as a result of these reactions, with a net shrinkage in 060 of up to 0.2% at 300 °C. The product at 300 °C has an X-ray pattern virtually identical to that of unoxidised glauconite.

2. Dehydroxylation, which occurs between about 300 and 600 °C, is accompanied by a further decrease in the 060 spacing. Changes in the Mössbauer spectra can be interpreted on the basis of a dehydroxylated structure similar to that of the dehydroxylates of related minerals (montmorillonite and muscovite), in which the octahedral layer has become five-coordinate, but also contains significant numbers of cations in four-fold and very distorted six-fold coordination.

3. On heating above the dehydroxylation temperature, the X-ray diffraction patterns and Mössbauer spectra broaden as a result of increased lattice disorder. At about 1000 °C, a spinel phase appears, the crystallinity of which increases at higher temperatures. The unit cell parameter and Mössbauer spectrum of this phase indicates that it is $MgFe_2O_4$ rather than Fe_3O_4, as

previously suggested [7,24]. At 1200 °C, the only other detectable crystalline phase is haematite (Fe_2O_3), the magnetic hyperfine field of which suggests the presence of substitutional Al. The silica and alkalis which separate during spinel formation appear in the high-temperature products as a glassy phase.

4. The chemical analyses and Mössbauer data for the present glauconites suggest a crystal structure in which both the *cis*- and *trans*-octahedral sites are occupied, the precise configuration depending on the chemical composition of the mineral, and on whether or not tetrahedral substitution is taken into account. The structures of dehydroxylated phases resulting from such models are fully consistent with the experimental data for glauconite dehydroxylate.

ACKNOWLEDGEMENTS

We are indebted to Dr. D.E. Rogers, N.J. Tapp and Mr. L.M. Parker for assistance with the thermal analyses.

REFERENCES

1 J.H. Johnston and C.M. Cardile, Clays Clay Miner., 35 (1987) 170; C.M. Cardile, Hyperfine Interact., 41 (1988) 767.
2 R.C. MacKenzie (Ed.), The Differential Thermal Investigation of Clays, Min. Soc. Monograph, London, 1957, Chapter 6.
3 T.A. Korneva and I.V. Nikolaeva, Tr. Inst. Geol. Geofiz., Akad. Nauk SSSR, Sib. Otd., 144 (1971) 132.
4 V.A. Logvinenko, I.V. Nikolaeva and M.Yu. Kameneva, Tr. Inst. Geol. Geofiz., Akad. Nauk SSSR, Sib. Otd., 610 (1985) 143.
5 K. Utsal and V. Utsal, Tartu Riikliku Ulik. Toim., 561 (1981) 50.
6 G.R. Thompson and J. Homer, Clays Clay Miner., 23 (1975) 289.
7 M. Escoubes, M. Murat, M.M. Karchoud and M. Charbonnier, Bull. Soc. Fr. Ceram., 100 (1973) 39.
8 M. Escoubes and M.M. Karchoud, Bull. Soc. Fr. Ceram., 114 (1977) 43.
9 A. Cimbalnikova, K. Raclavsky and J. Lipka, in J. Konta (Ed.), Proc. 6th Conf. Clay Mineral. Petrol., Prague, 1973, Jiri. Univ. Karlova, Prague, 1975, p. 57.
10 K. Raclavsky, J. Sitek and J. Lipka, in M. Huel and T. Zemcik (Ed.), Proc. 5th Int. Conf. Mössbauer Spectroscopy, Prague, 1973, 1975, p. 368.
11 H. Annersten, Neues Jahrb. Mineral., Monatsh., 8 (1975) 378.
12 M.V. Eirish and A.A. Dvorechenskaya, Geokhimiya, 5 (1976) 748.
13 R.M. Rolf, C.W. Kimball and I.E. Odom, Clays Clay Miner., 25 (1977) 131.
14 V.S. Grechishkin, K.P. Zangalis, I.V. Murin, E.M. Emel'yanov, V.P. Sivkov and G.S. Kharin, Izv. Akad. Nauk SSSR, Ser. Fiz., 42 (1978) 2654.
15 I. Rozenson and L. Heller-Kallai, Clays Clay Miner., 26 (1978) 173.
16 D.M. McConchie, J.B. Ward, V.H. McCann and D.W. Lewis, Clays Clay Miner., 27 (1979) 339.

17 A. Govaert, E. De Grave, H. Quartier, D. Chambaere and G. Robbrecht, J. Phys., Colloq. (Orsay), 2 (1979) 442.
18 C.A.M. Ross and G. Longworth, Clays Clay Miner., 28 (1980) 43.
19 A. Kotlicki, J. Szczyrba and A. Wiewiora, Clay Miner., 16 (1981) 221.
20 Kh. I. Amirkhanov, L.K. Anokhina, R.U. Gabitova, I.V. Nikolaeva and R.I. Chalabov, Dokl. Akad. Nauk SSSR, 275 (1984) 967.
21 E. De Grave, J. Vandenbruwaene and E. Elewaut, Clay Miner., 20 (1985) 171.
22 E.E. Kohler and H.M. Koster, Clay Miner., 11 (1976) 273.
23 L.G. Daynyak and V.A. Drits, Clays Clay Miner., 35 (1987) 363.
24 N.M. Jamthe, A. Krishnamurthy, B.K. Srivastava and S. Lokanathan, Proc. Nucl. Phys. Solid-State Phys. Symp. 1982, 25C (1984) 191.
25 C.M. Cardile and I.W.M. Brown, Clay Miner., 23 (1988) 13.
26 K.J.D. MacKenzie and M.E. Bowden, Thermochim. Acta, 64 (1983) 83.
27 I.W.M. Brown, K.J.D. MacKenzie and R.H. Meinhold, J. Mater. Sci., 22 (1987) 3265.
28 K.J.D. MacKenzie, I.W.M. Brown, C.M. Cardile and R.H. Meinhold, J. Mater. Sci., 22 (1987) 2645.
29 L. Heller-Kallai and I. Rozenson, Clays Clay Miner., 28 (1980) 355.
30 E. De Grave, A. Govaert, D. Chambaere and G. Robbrecht, Physica B, 96 (1979) 103.
31 C.W. Childs and J.G. Baker-Sherman, NZ Soil Bureau Sci. Rep. 66, DSIR, 1984.
32 A.P. Zhukhlistov, B.B. Zyvagin, E.K. Lazarenko and V.I. Pavlishin, Sov. Phys. Crystallogr., 22 (1977) 284.
33 S.I. Tsipursky and V.A. Drits, Clay Miner., 19 (1984) 177.